Original Article



# Local lung deposition of ultrafine particles in healthy adults: experimental results and theoretical predictions

**Robert Sturm**

Department of Materials Science and Physics, Division of Physics and Biophysics, University of Salzburg, Salzburg, Austria
*Correspondence to:* Dr. Robert Sturm. Brunnleitenweg 41, A-5061 Elsbethen, Austria. Email: sturm_rob@hotmail.com.

**Background:** Ultrafine particles (UFP) of biogenic and anthropogenic origin occur in high numbers in the ambient atmosphere. In addition, aerosols containing ultrafine powders are used for the inhalation therapy of various diseases. All these facts make it necessary to obtain comprehensive knowledge regarding the exact behavior of UFP in the respiratory tract.

**Methods:** Theoretical simulations of local UFP deposition are based on previously conducted inhalation experiments, where particles with various sizes (0.04, 0.06, 0.08, and 0.10 µm) were administered to the respiratory tract by application of the aerosol bolus technique. By the sequential change of the lung penetration depth of the inspired bolus, different volumetric lung regions could be generated and particle deposition in these regions could be evaluated. The model presented in this contribution adopted all parameters used in the experiments. Besides the obligatory comparison between practical and theoretical data, also advanced modeling predictions including the effect of varying functional residual capacity (FRC) and respiratory flow rate were conducted.

**Results:** Validation of the UFP deposition model shows that highest deposition fractions occur in those volumetric lung regions corresponding to the small and partly alveolated airways of the tracheobronchial tree. Particle deposition proximal to the trachea is increased in female probands with respect to male subjects. Decrease of both the FRC and the respiratory flow rate results in an enhancement of UFP deposition.

**Conclusions:** The study comes to the conclusion that deposition of UFP taken up via bolus inhalation is influenced by a multitude of factors, among which lung morphometry and breathing conditions play a superior role.

**Keywords:** Deposition model; ultrafine particles (UFP); inhalation experiments; aerosol bolus; volumetric lung region; therapeutic aerosol

Submitted Sep 26, 2016. Accepted for publication Oct 10, 2016.
doi: 10.21037/atm.2016.11.13
**View this article at:** http://dx.doi.org/10.21037/atm.2016.11.13

## Introduction

Although ultrafine particles (UFP), which commonly adopt diameters <0.1 µm, have a total mass remaining under that of coarse particulate matter by several orders of magnitude, they occur in much greater number in the ambient atmosphere. Additionally, they are characterized by a large surface area to mass ratio with respect to their coarse counterparts, so that they can act as potential carriers of harmful gaseous compounds (1). Possible health effects of UFP have been studied first on laboratory animals (2,3). These experimental investigations have come to the conclusion that animals exposed to high doses of UFP are subject to an enhanced risk for non-lethal and lethal lung injuries. Epidemiological research conducted in the late 1990s could demonstrate that UFP transported in the urban air produce greater adverse respiratory effects than particles adopting diameters >0.1 µm (1,4). Meanwhile, scientific activity has increasingly focused on those molecular and cellular mechanisms standing behind the unwholesome behavior of UFP (5-8). Here, it could be among other found out that UFP are, directly or indirectly, responsible for the generation of free radicals (ROS, RNS), which are able to influence processes taking place on the DNA (7). Furthermore, UFP have the ability to pass epithelial barriers within extremely short periods of time (8,9), which enables their rapid accumulation in blood capillaries with all

its after-effects.

In order to obtain a detailed insight into local respiratory effects of UFP in humans, exposure-dose relationships are of indispensable value. Collection of related experimental data already started in the 1980s, with healthy male adults acting as preferred test subjects (10-12). In the following decades respective research was also extended on patients with obstructive lung diseases (13,14), children (15), and healthy female adults (16,17). Early studies on UFP inhalation were characterized by small, non-representative numbers of test subjects, high size variations of the used aerosol particles, and arbitrary selection of the particulate material (oils, salts, soot, metals) (1). Since the 2000s, however, generation of aerosols including UFP has taken place according to better and more standardized procedures, so that generalization of the collected data to the whole population has been enabled (18).

Since the1970s numerous inhalation experiments have been accompanied by related theoretical computations. The formulation of models dealing with particle inhalation and deposition has become necessary in order to increase the understanding of all those physical effects that are responsible for the transport behavior of particulate matter in specific lung structures. Serious simulation of UFP inhalation began in the 1990s and included both contemporary experimental findings and current considerations with regard to the generation of a close-to-reality lung architecture (9,18). This modeling approach has been subjected to numerous validation processes and may be evaluated as highly reliable in the meantime.

The present contribution pursues three main objectives: (I) the local deposition of UFP delivered in the lungs with the help of the aerosol bolus technique is approximated theoretically, and generated results are compared with experimental data (18); (II) hypothetical aerosol bolus inhalation of UFP is extended to different lung sizes, expressed by the functional residual capacity (FRC), and velocities of aerosol inhalation (respiratory flow rate Q); (III) possible effects controlling local UFP deposition are subjected to a comprehensive debate.

## Methods

### *Experimental setup*

Experiments included 22 adult test subjects (11 men and 11 women) who ranged in age from 20 to 40 years. Mean FRC of the male probands amounted to 3,911±892 mL, whereas that of the female probands assumed a value of 3,314±547 mL. All test subjects underwent a comprehensive physical and medical examination, and only persons, who had passed this initial screening, were admitted to the inhalation experiments (1,18).

Generation of ultrafine aerosol particles took place by condensing sebacate oil vapour on non-hygroscopic nuclei of metal particles. The monodisperse aerosols emerging from the respective aerosol generator were diluted with filtered air and forwarded to the inhalation device. For the experimental work particles with number median diameters (NMD) of 0.04, 0.06, 0.08, and 0.10 µm as well as geometric standard deviations ($\sigma_g$) ranging from 1.27 to 1.34 were generated.

Aerosol inhalation was conducted by application of the aerosol bolus technique, where defined aerosol volumes (in the concrete case 45 mL) are injected into the inhaled air stream at predefined time points. By changing the injection time point, aerosol transported within the bolus was delivered to different lung depths. In the experiments described here single probands inhaled the aerosol bolus with a tidal volume ($V_T$) of 500 mL at a respiratory flow rate of 250 mL·s$^{-1}$, resulting in an inhalation time of 2 s. Lung penetration depth ($V_p$) of the inhaled aerosol boluses ranged from 50 to 500 mL and was changed in 50 mL increments by using a specific method of sequential aerosol inhalation. For each inspiration experiment the number of particles inhaled ($N_{in}$) and subsequently exhaled ($N_{ex}$) was computed and thereupon the related recovery rate (RC) was calculated according to the formula

$$RC = N_{ex}/N_{in}. \quad [1]$$

Local particle deposition efficiency ($X_i$), describing the deposition fraction of particulate matter at a given lung penetration depth ($V_{p,i}$) was determined with the help of the mathematical equation (18)

$$X_i = 1 - (RC_i / RC_{i-1})^{0.5} = 1 - [(N_{ex,i} / N_{in,i})/(N_{ex,i-1} / N_{in,i-1})]^{0.5} \quad [2]$$

### *Modeling ultrafine particle deposition*

Simulation of the inhalation experiments was conducted by using the aerosol bolus subroutine of the stochastic particle transport and deposition code IDEAL which was originally developed by Koblinger and Hofmann at the end of the 1980s (19,20). The program is based on the assumption of random particle transport within a stochastic lung architecture. Such a structure of the tracheobronchial tree is commonly characterized by morphometric variability of

 

the bronchial and bronchiolar tubes within a given airway generation. This generation-specific intrasubject variability was realized by using generation-related probability density functions of diverse geometric parameters. Selection of data from these functions was carried out by using the random number concept. Each particle inhaled through the mouth or nose and passing the trachea followed an individual path, whose course was based on both randomness and the volume fractions of inhaled air splitted at bronchial and bronchiolar bifurcations. With the help of the Monte Carlo technique high numbers of particle transport and deposition events were generated simultaneously and submitted to an appropriate statistical evaluation.

Theoretical generation of aerosol pulses with given volume, which are injected into the inhaled air stream at predefined time points, requires the input of bolus half-width and lung penetration depth in terms of time values standardized to the duration of the inhalation event. For an inhalation time ($t_{in}$) of 2 s (see above) and a tidal volume of 500 mL, an aerosol bolus half-width of 45 mL corresponds to a time interval of 0.18 s. A lung penetration depth of 50 mL, on the other hand, requires the hypothetical inhalation of the bolus at 1.8 s. In general, transformation between time and volume data may be realized by the formulae

$$t_{bw} = (t_{in}/V_p) \cdot V_{bw} \quad [3]$$

and

$$t_{Vp} = t_{in} - (t_{in}/V_p) \cdot V_{Vp}, \quad [4]$$

where $t_{bw}$, $t_{Vp}$, $V_{bw}$, and $V_{Vp}$, respectively, denote the time measures of bolus half-width and lung penetration depth as well as the volume measures of these two parameters. Mathematical generation of the bolus peak takes place by assuming either a Gaussian particle distribution or a rectangular distribution within the inspired aerosol pulse. The distal end of the bolus is evaluated by application of a Newtonian approach. As stated in detail elsewhere (21-24), change of aerosol bolus shape and position during its transport through the pulmonary structures represents an essential phenomenon that may be approximated by diverse momentum-based parameters (standard deviation, skewness, mode-shift).

Deposition of UFP was simulated by assuming three principal deposition mechanisms (Brownian motion, inertial impaction, gravitational settling), among which only diffusion-related collision of particulate matter with the airway walls may be evaluated as highly significant for the particle sizes considered here. Estimation of particle fractions deposited in single lung compartments, whose range had been defined by lung penetration depth (see above), was based on analytical and empirical formulae described in detail elsewhere (19,25-29). In the present model any deposition effects emerging from phoretic processes were evaluated as negligible (30), since sebacate particles may be considered as largely uncharged and differences in temperature between inhaled and residual air are already handled in part by the Einstein diffusion coefficient.

## Results

### *Comparison between experimental and theoretical data*

Deposition of particles adopting a diameter of 0.04 µm depends on the lung penetration depth insofar as a starting value for $V_p$ of 50 mL commonly produces small deposition fractions, increase of $V_p$ from 50 to 150 mL results in a remarkable enhancement of the deposition fractions, and with any further increase of $V_p$ deposition is again subject to a continuous decline (*Figure 1*). As found by experimental work, in male subjects particle deposition fraction initially amounts to 0.003 ($V_p$=50 mL), reaches a maximum value of 0.115 ($V_p$=150 mL) and decreases to 0.010 ($V_p$=500 mL). In female subjects respective deposition fractions adopt values of 0.029, 0.117, and 0.010. Modeling predictions including a statistical unsharpness of 10% to 15% are in good correspondence with the experimental results, with highest deviations being noticeable for $V_p$>200 mL.

In the case of particles with a diameter of 0.06 µm tendencies of local particle deposition are quite similar to those noted for 0.04 µm particles (*Figure 2*), but deposition fractions are reduced by about 50%. In male subjects local deposition rises from 0.002 ($V_p$=50 mL) to 0.064 ($V_p$=200 mL) and after that declines again to 0.010 ($V_p$=500 mL). In females, the initial deposition value amounts to 0.022 ($V_p$=50 mL), whereas the maximum value is 0.072 ($V_p$=150 mL) and the terminal value is 0.009 ($V_p$=500 mL). Modeling predictions exhibit a partly excellent correspondence with the experimental results, with almost all practical data plotting within the unsharpness interval of the theoretical predictions. Again, predictive accuracy slightly declines with increasing $V_p$.

Aerosol particles with a diameter of 0.08 µm assume local deposition fractions of 0.002 ($V_p$=50 mL), 0.056 ($V_p$=200 mL), and 0.010 ($V_p$=500 mL) in male probands. In female probands marginal and maximum deposition fractions amount to 0.020

 

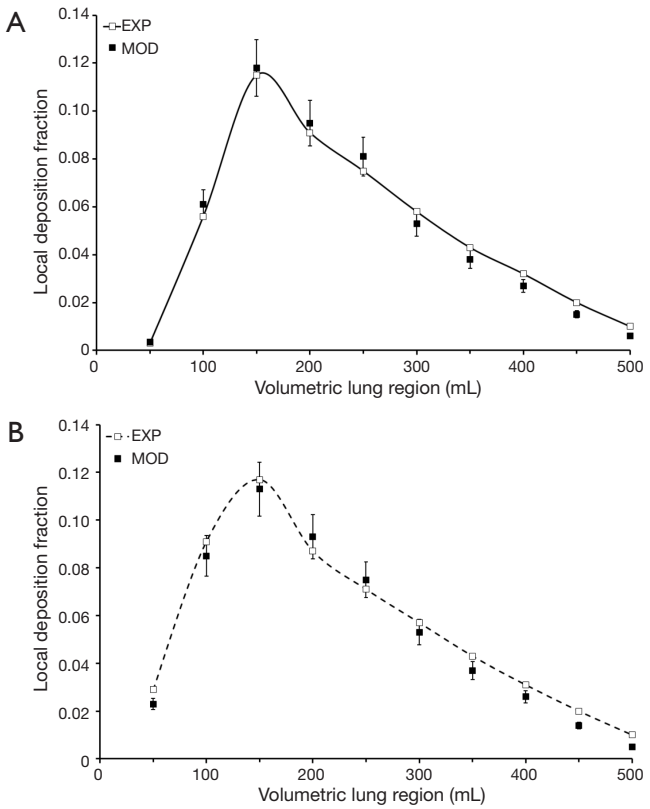


**Figure 1** Experimental and theoretical data (mean ± standard deviation) of local deposition fractions of particles measuring 0.04 µm in size after aerosol bolus inhalation: (A) males; (B) females.

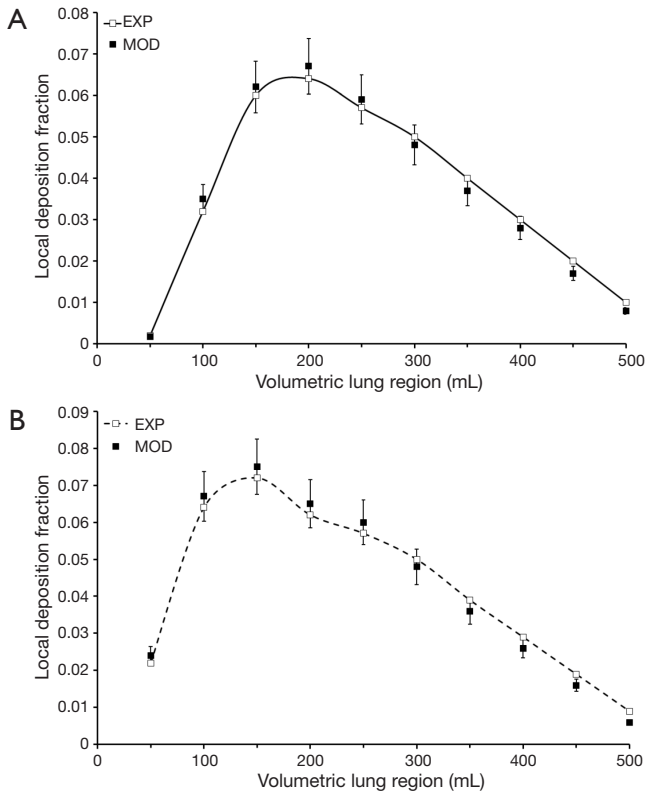


**Figure 2** Experimental and theoretical data (mean ± standard deviation) of local deposition fractions of particles measuring 0.06 µm in size after aerosol bolus inhalation: (A) males; (B) females.

($V_p$=50 mL), 0.055 ($V_p$=150 mL), and 0.010 ($V_p$=500 mL). Differences between hypothetical and experimental results are on the order of several percent in the case of both males and females, with highest discrepancies occurring at intermediate values of $V_p$ (*Figure 3*).

Regarding aerosol particles with a diameter of 0.10 µm deposition fraction measured in male subjects increases from 0.002 ($V_p$=50 mL) to 0.042 ($V_p$=200 mL) first and afterwards declines again to a terminal value of 0.007. In female probands particle deposition fraction develops from 0.005 ($V_p$=50 mL) to 0.045 ($V_p$=150 mL) and assumes a terminal value of 0.007 ($V_p$=500 mL). For this particle size differences between predicted and measured values of local particle deposition fractions exhibit a maximum of 10% and thus confirm the high modeling accuracy already reported for smaller particles (*Figure 4*).

Experimental measurements and related predictions of regional particle deposition fractions (head, tracheobronchial region, alveolar region; values are given in percent) are summarized in *Figures 5* and *6*. Comparison of male and female subjects clearly shows that women are commonly characterized by higher particle deposition in the head and tracheobronchial region with respect to men, whereas men surpass women with regard to alveolar deposition. These trends are in great parts retraced by the modeling approach. In general all regional deposition fractions are subject to a permanent decline with increasing particle size, so that 0.10 µm particles perform a deposition being about half as high as that recognized for 0.04 µm particles.

### *Advanced modeling predictions*

Further modeling predictions have been carried out in order to answer two main questions: (I) how does deposition of UFP taken up into the respiratory tract by bolus inhalation change with varying FRC, being a measure for lung size? (II) Which effects on particle deposition have to be expected by modifying the respiratory flow rate?

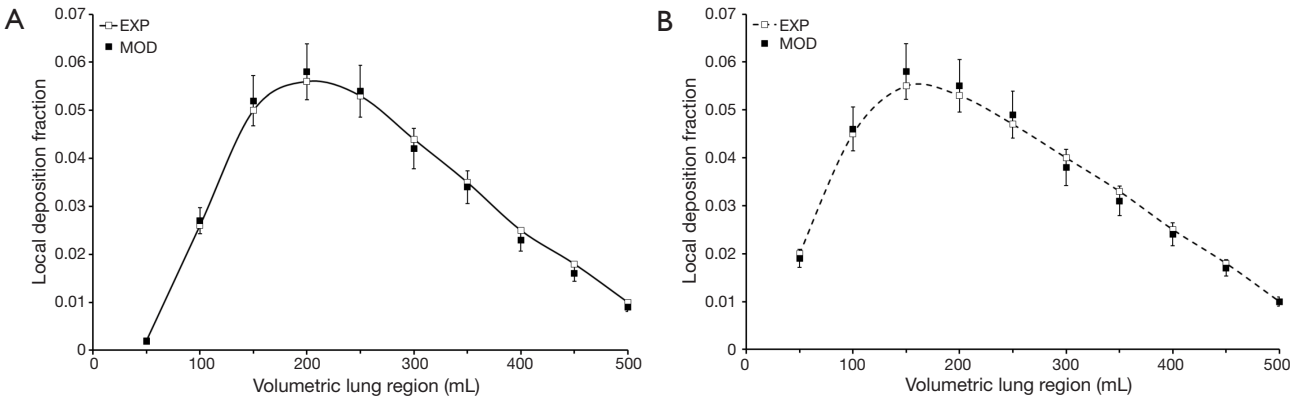


**Figure 3** Experimental and theoretical data (mean ± standard deviation) of local deposition fractions of particles measuring 0.08 μm in size after aerosol bolus inhalation: (A) males; (B) females.

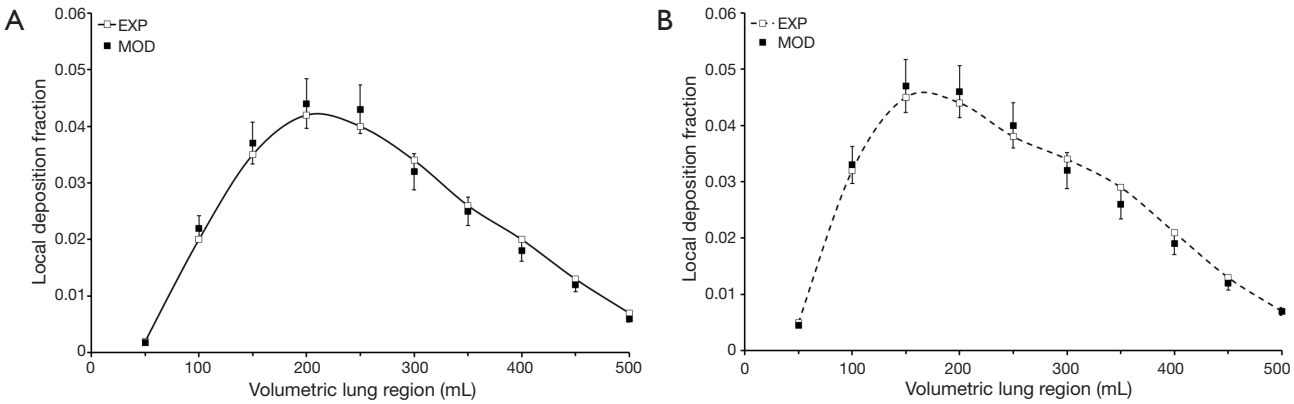


**Figure 4** Experimental and theoretical data (mean ± standard deviation) of local deposition fractions of particles measuring 0.10 μm in size after aerosol bolus inhalation: (A) males; (B) females.

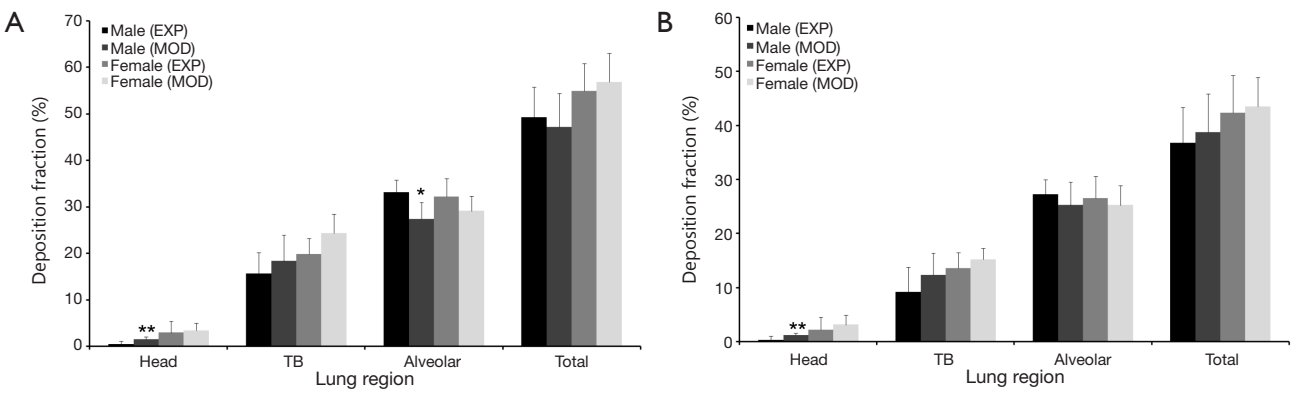


**Figure 5** Experimental and theoretical results (mean ± standard deviation) of regional particle deposition fractions in male and female subjects: (A) 0.04-μm particles; (B) 0.06-μm particles. Asterisks indicate significant (*, P<0.05) or highly significant (**, P<0.001) differences between experiment and model.

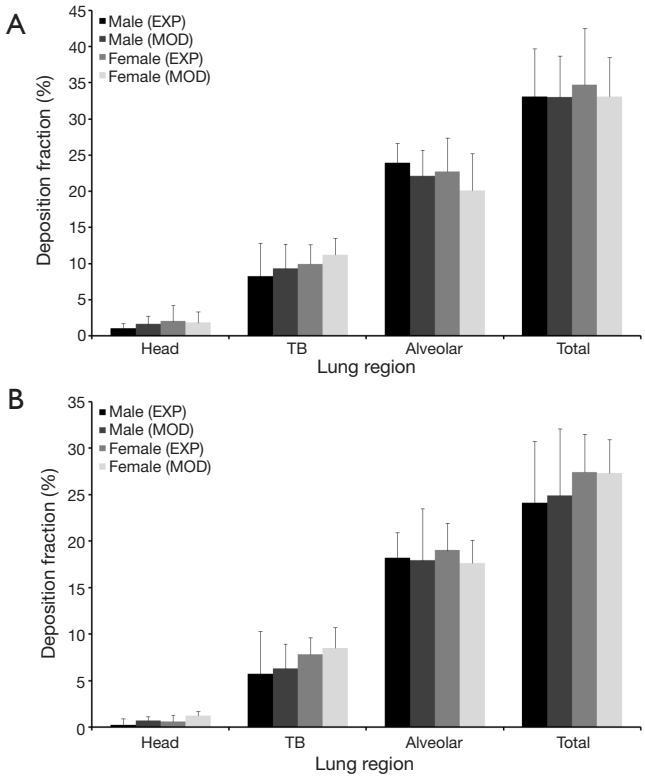


**Figure 6** Experimental and theoretical results (mean ± standard deviation) of regional particle deposition fractions in male and female subjects: (A) 0.08-µm particles; (B) 0.10-µm particles.

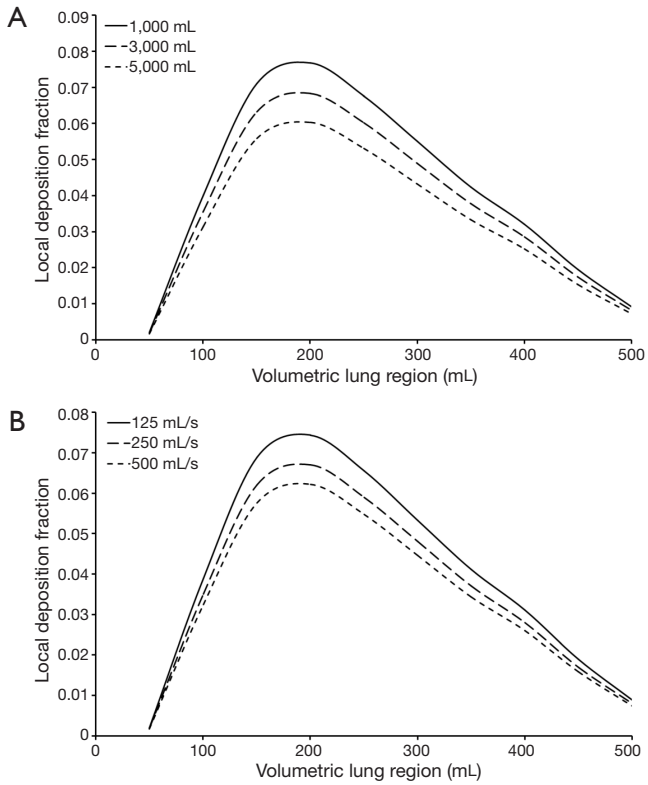


**Figure 7** Advanced modeling predictions: (A) effect of functional residual capacity (FRC) on local deposition fractions of 0.06-µm particles; (B) influence of respiratory flow rate (Q) on local deposition fractions of 0.06-µm particles (FRC =3,000 mL).

Regarding the variation of the FRC, main results obtained from the model are summarized in *Figure 7A*. Starting at 5,000 mL this parameter was continuously decreased in 2,000 mL steps, until a minimum value of 1,000 mL was attained. Since the parameter may be regarded as reliable measure of lung size, each value exhibited in the related graph corresponds with a specific developmental stage of the respiratory tract (24-26,31). Calculations were limited to particles assuming a size of 0.06 µm. From the diagram the clear tendency of increasing deposition values with any reduction of the FRC can be discerned. In the concrete case of the studied particle size, local deposition values are raised by maximal 25%, when FRC is reduced from 5,000 to 1,000 mL. Maximum deposition occurring for a lung penetration depth of 150 mL amounts 0.060 after assumption of high FRC, but to 0.077 in the case of low FRC.

Modification of the respiratory flow rate has an effect on local deposition of 0.06 µm particles insofar as any prolongation of inhalation time and associated maintenance of the tidal volume results in a measurable increase of the deposition values, whereas acceleration of inspiration is accompanied by a decrease of particle deposition (*Figure 7B*). In concrete terms, a reduction of the respiratory flow rate by 50% (125 mL·s$^{-1}$) leads to an average enhancement of local deposition values by up to 12%. An elevation of the flow rate by 100% (500 mL·s$^{-1}$) is characterized by an average diminution of local deposition by up to 9%.

## Discussion and conclusions

According to experimental and epidemiological studies, inhaled UFP bear an increased capability to act as triggers of numerous pulmonary insufficiencies (5-8,10-18). Therefore, every increase of our knowledge concerning the behavior of such particles in the different compartments of the respiratory system implies a crucial progress in medical science. This development is attained by both

the execution of practical measurements on preselected subjects and the definition of appropriate particle transport and deposition models. In the study presented here an ideal symbiosis between experiment and model could be demonstrated insofar as both approaches yielded very similar results with regard to the local, aerosol bolus-related deposition of particles ranging in size from 0.04 to 0.10 µm. Good correspondence between experiment and model may be regarded as a result of continuous validation of the theoretical approach during the past 20 years (25-30). On the other hand, any derivation of local deposition data from a sequence of inhaled aerosol boluses (18) is accompanied by several sources of inaccuracy, since all frame conditions adjusted for the inhalation procedure have to be kept as stable as possible. Even small deviations of the parameters $N_{ex}$ and $N_{in}$ introduced in Eq. [1] and [2] have a significant effect on the calculated local deposition fractions $X_i$.

According to the experimental and theoretical data, highest particle deposition is measured in that lung compartment which is defined by a lung penetration volume ranging from 150 to 200 mL. From an anatomical point of view this volumetric lung region primarily covers the small ciliated airways of the bronchiolar lung region which are not fully alveolated yet (31-39). Within the fine tubular network, Brownian motion advances to that mechanism being most essential for the collision of particulate substances with the airway walls (28-30). In the volumetric lung region posited closer to the trachea, airway diameters are about one order of magnitude larger than those in the bronchiolar region, so that efficiency of Brownian motion exerting on the inhaled particles is significantly diminished. In the more distal lung regions ($V_p$>200 mL) UFP are increasingly forced to enter the aveoli. Here, partly incomplete mixing processes between inhaled particle-loaded air on the one side and residual alveolar air on the other cause that small particles are remarkably hindered to hit the epithelial wall (7,9,25).

As demonstrated in *Figures 1-6*, particles measuring 0.10 µm in size commonly produce local and regional deposition fractions which are about half as high as those resulting from the inhalation of 0.04 mm particles. This negative correlation between particle diameter and deposition efficiency was already described in detail in numerous previous studies (7,25-29) and has to interpreted as result of the particle size dependence of the Einsteinian diffusion coefficient. According to the respective formula describing particle diffusion in a gaseous system, an increase in particle size by the factor 10 corresponds to a reduction of the parameter by a factor of 100. In this context, differences in particle deposition behavior between male and female probands are of enhanced interest. According to the deposition graphs described in the preceding chapter extrathoracic and tracheobronchial particle deposition generally adopt higher values in women than in man, whereas for alveolar deposition a reverse phenomenon may be observed. In this case the relationship between diffusion-related deposition and airway morphometry becomes highly evident insofar as smaller calibers of the extrathoracic and tracheobronchial airways, which are realized in female lungs, produce higher local and regional deposition fractions. Enhanced deposition of UFP in the air conducting zone of the respiratory tract has the consequence that lower numbers of particles reach the alveoli, where they hit the epithelial walls with the same probability as in the male lungs (26-31).

As found by theoretical simulations concerning local deposition of 0.06 µm particles, any decrease in FRC, corresponding to a diminution of lung size, results in enhanced deposition fractions. This phenomenon can be explained by the fact that based on the findings outlined for the female respiratory tract any further reduction of the airway calibers and simultaneous maintenance of the breathing parameters lead to higher tracheobronchial penetration depths of the inspired particulate mass and an intensification of diffusive deposition. In the lungs of children and adolescents, which are characterized by functional residual capacities ranging from 1,000 to 2,000 mL, this effect becomes particularly clear, and any further reduction of lung size (young children, infants) would imply a maximization of diffusion-related particle deposition in the air-conducting zone, but a minimization of the exhaled particle fraction (30,31). As already stated for the female respiratory system, the airway architecture of the upper respiratory system acts as a kind of particle filter under respective inhalation conditions which hinders the generation of high surface-related particle doses in the distal lung and therefore reduces the probability of particle-induced lung insufficiencies (32-39).

Increase in respiratory flow rate is commonly accompanied by a reduction of local and regional deposition (*Figure 7B*) which may be explained by the fact that shortening of particle residence time in the lung airways reduces the lateral transport distances performed by the particles due to Brownian motion. On the other hand, these increments of lateral particle dislocation are added from one airway generation to the next, so that deposition

 

events increasingly take place in more distal parts of the tracheobronchial tree. Extreme enhancement of the flow rate, however, causes the main exhalation of the particulate mass, before its deposition can be initiated (7,9,19,20).

From the results presented in this study it may be concluded that deposition of UFP taken up via bolus inhalation is influenced by a multitude of factors, among which lung morphometry and breathing conditions play a superior role. This information obtained from both experimental and theoretical work is of enhanced value in several aspects: (I) numerous modern inhalation therapies use ultrafine powder aerosols that should reach their target regions in high concentrations. Here, additional notes regarding an optimized setup of the inhalator are highly welcome; (II) many environmental particles fall within the size range of UFP, so that development of certain breathing practices may help to reduce the amount of uptaken particulate mass.

## Acknowledgements

None.

## Footnote

*Conflicts of Interest*: The author has no conflicts of interest to declare.

## References

1. Jaques PA, Kim CS. Measurement of total lung deposition of inhaled ultrafine particles in healthy men and women. Inhal Toxicol 2000;12:715-31.
2. Oberdorster G, Gelein RM, Ferin J, et al. Association of particulate air pollution and acute mortality: involvement of ultrafine particles? Inhal Toxicol 1995;7:111-24.
3. Li N, Sioutas C, Cho A, et al. Ultrafine particulate pollutants induce oxidative stress and mitochondrial damage. Environ Health Perspect 2003;111:455-60.
4. Oberdörster G, Ferin J, Gelein R, et al. Role of the alveolar macrophage in lung injury: studies with ultrafine particles. Environ Health Perspect 1992;97:193-9.
5. Donaldson K, Tran CL. Inflammation caused by particles and fibers. Inhal Toxicol 2002;14:5-27.
6. Schins RP, Lightbody JH, Borm PJ, et al. Inflammatory effects of coarse and fine particulate matter in relation to chemical and biological constituents. Toxicol Appl Pharmacol 2004;195:1-11.
7. Sturm R. Theoretical and experimental approaches to the deposition and clearance of ultrafine carcinogens in the human respiratory tract. Thorac Cancer 2011;2:61-8.
8. Seaton A, MacNee W, Donaldson K, et al. Particulate air pollution and acute health effects. Lancet 1995;345:176-8.
9. Hofmann W, Sturm R, Winkler-Heil R, et al. Stochastic model of ultrafine particle deposition and clearance in the human respiratory tract. Radiat Prot Dosimetry 2003;105:77-80.
10. Blanchard JD, Willeke K. Total deposition of ultrafine sodium chloride particles in human lungs. J Appl Physiol Respir Environ Exerc Physiol 1984;57:1850-6.
11. Wilson FJ Jr, Hiller FC, Wilson JD, et al. Quantitative deposition of ultrafine stable particles in the human respiratory tract. J Appl Physiol (1985) 1985;58:223-9.
12. Schiller CF, Gebhart J, Heyder J, et al. Factors influencing total deposition of ultrafine aerosol particles in the human respiratory tract. J Aerosol Sci 1986;17:328-32.
13. Anderson PJ, Wilson JD, Hiller FC. Respiratory tract deposition of ultrafine particles in subjects with obstructive or restrictive lung disease. Chest 1990;97:1115-20.
14. Brown JS, Zeman KL, Bennett WD. Ultrafine particle deposition and clearance in the healthy and obstructed lung. Am J Respir Crit Care Med 2002;166:1240-7.
15. Sturm R. Theoretical models of carcinogenic particle deposition and clearance in children's lungs. J Thorac Dis 2012;4:368-76.
16. Bennett WD, Zeman KL, Kim C. Variability of fine particle deposition in healthy adults: effect of age and gender. Am J Respir Crit Care Med 1996;153:1641-7.
17. Kim CS, Hu SC, Ding J. Deposition distribution of inhaled particles in healthy human lungs: Comparative studies for ultrafine, fine and coarse particles. Am J Respir Crit Care Med 1998;157:A474.
18. Kim CS, Jaques PA. Analysis of total respiratory deposition of inhaled ultrafine particles in adult subjects at various breathing patterns. Aerosol Sci Technol 2004;38:525-40.
19. Koblinger L, Hofmann W. Monte Carlo modeling of aerosol deposition in human lungs. Part I: Simulation of particle transport in a stochastic lung structure. J Aerosol Sci 1990;21:661-74.
20. Koblinger L, Hofmann W. Analysis of human lung morphometric data for stochastic aerosol deposition calculations. Phys Med Biol 1985;30:541-56.
21. Sturm R, Pawłak E, Hofmann W. Monte-Carlo-Model for the aerosol bolus dispersion in the human lung--part 1: theoretical model description and application. Z Med Phys 2007;17:127-35.

 

22. Sturm R, Pawłak E, Hofmann W. Monte-Carlo-Model for the aerosol bolus dispersion in the human lung--part 2: model predictions for the diseased lung. Z Med Phys 2007;17:136-43.
23. Hofmann W, Pawlak E, Sturm R. Semi-empirical stochastic model of aerosol bolus dispersion in the human lung. Inhal Toxicol 2008;20:1059-73.
24. Sturm R. Aerosol bolus dispersion in healthy and asthmatic children-theoretical and experimental results. Ann Transl Med 2014;2:47.
25. Sturm R, Hofmann W. A theoretical approach to the deposition and clearance of fibers with variable size in the human respiratory tract. J Hazard Mater 2009;170:210-8.
26. Sturm R. Theoretical deposition of nanotubes in the respiratory tract of children and adults. Ann Transl Med 2014;2:6.
27. Sturm R. Nanotubes in the human respiratory tract - Deposition modeling. Z Med Phys 2015;25:135-45.
28. Sturm R. Spatial visualization of theoretical nanoparticle deposition in the human respiratory tract. Ann Transl Med 2015;3:326.
29. Sturm R. A stochastic model of carbon nanotube deposition in the airways and alveoli of the human respiratory tract. Inhal Toxicol 2016;28:49-60.
30. Sturm R. Inhaled nanotubes. Physics Today 2016;69:70-1.
31. International Commission on Radiological Protection (ICRP). Human respiratory tract model for radiological protection. Publication 66. Oxford: Pergamon Press, 1994.
32. Hofmann W, Sturm R. Stochastic model of particle clearance in human bronchial airways. J Aerosol Med 2004;17:73-89.
33. Sturm R, Hofmann W. A multi-compartment model for slow bronchial clearance of insoluble particles--extension of the ICRP human respiratory tract models. Radiat Prot Dosimetry 2006;118:384-94.
34. Sturm R. A computer model for the clearance of insoluble particles from the tracheobronchial tree of the human lung. Comput Biol Med 2007;37:680-90.
35. Sturm R. A three-dimensional model of tracheobronchial particle distribution during mucociliary clearance in the human respiratory tract. Z Med Phys 2013;23:111-9.
36. Sturm R, Hofmann W, Scheuch G, et al. Particle Clearance in Human Bronchial Airways: Comparison of Stochastic Model Predictions with Experimental Data. Ann Occup Hyg 2002;46:329-33.
37. Sturm R, Hofmann W. Stochastic modeling predictions for the clearance of insoluble particles from the tracheobronchial tree of the human lung. Bull Math Biol 2007;69:395-415.
38. Sturm R. Age-dependence and intersubject variability of tracheobronchial particle clearance. Pneumon 2011;24:77-85.
39. Sturm R. An advanced stochastic model for mucociliary particle clearance in cystic fibrosis lungs. J Thorac Dis 2012;4:48-57.

**Cite this article as:** Sturm R. Local lung deposition of ultrafine particles in healthy adults: experimental results and theoretical predictions. Ann Transl Med 2016;4(21):420. doi: 10.21037/atm.2016.11.13

 